

Modifications to Swisdak (2013)'s rejection sampling algorithm for a Maxwell–Jüttner distribution in particle simulations

Seiji Zenitani¹

Space Research Institute, Austrian Academy of Sciences, 8042 Graz, Austria^{a)}

Modifications to Swisdak [Phys. Plasmas **20**, 062110 (2013)]'s rejection sampling algorithm for drawing a Maxwell–Jüttner distribution in particle simulations are presented. Handy approximations for e -folding points and a linear slope in the envelope function are proposed, to make the algorithm self-contained and more efficient.

In kinetic plasma simulations such as particle-in-cell (PIC) and Monte Carlo simulations, it is often necessary to initialize particle velocities that follows a certain velocity distribution, by using random numbers (random variates). A relativistic Maxwell distribution, also known as a Maxwell–Jüttner distribution,² is one of the most important velocity distributions, in particular in high-energy astrophysics and in laser physics. Owing to its importance in modeling, Monte Carlo algorithms for drawing a Maxwell–Jüttner distribution have been developed over many years^{3,4} (see Ref. 4 and references therein).

In the article by Swisdak³, the author proposed an acceptance-rejection algorithm for a Maxwell–Jüttner distribution. Devroye¹'s piecewise method for log-concave distributions was applied. The algorithm is simple and efficient, as will be shown in this paper. Technically, it requires an external solver to find e -folding points, where the density is $1/e$ ($= 1/2.71828\dots$) of the maximum. This may not be ideal in some applications — for example, when the plasma temperature varies from grid cell to cell, it is necessary to repeatedly call the root finder, and the user may desire a simpler option. In this research note, we propose two modifications to Swisdak³'s sampling method. We propose handy approximations for the e -folding points and a linear slope in the envelope function to improve the acceptance efficiency.

First we recap Swisdak's application of the Devroye method. We limit our attention to an isotropic stationary population. In the spherical coordinates, the Maxwell–Jüttner distribution is given by

$$f(p) = Ap^2 \exp\left(-\frac{\sqrt{1+p^2}}{t}\right) \quad (1)$$

where A is the normalization constant, $p = m\gamma v$ is the momentum, v the velocity, $\gamma = [1 - (v/c)^2]^{-1/2} = [1 + (p/mc)^2]^{1/2}$ the Lorentz factor, and $t = T/mc^2$ the temperature. For simplicity, we set $m = c = 1$. A detail form of the normalization constant is found in many literature,⁴ but this article does not rely on it. The black curve in Fig. 1 shows the distribution function with $t = 1$. It has a maximum $f_m = f(p_m)$ at $p_m = [2t(t + \sqrt{1+t^2})]^{1/2}$. The rejection algorithm uses

a piecewise envelope function $F(p)$ of two exponential tails and a flat line, as shown in orange in Fig. 1.

$$F(p) = \begin{cases} f(p_L) \exp\left(\frac{p-p_L}{\lambda_L}\right) & (p \leq x_L) \\ f_m & (x_L < p \leq x_R) \\ f(p_R) \exp\left(-\frac{p-p_R}{\lambda_R}\right) & (x_R < p) \end{cases} \quad (2)$$

Here, the exponential tails touch the distribution function at $p = p_L$ and p_R , $\lambda_X = |f(p_X)/f'(p_X)|$ is the scale length at $p = p_X$ ($X=L, R$), and the two switching points are located at

$$x_L = p_L + \lambda_L \log \frac{f_m}{f(p_L)}, \quad x_R = p_R - \lambda_R \log \frac{f_m}{f(p_R)} \quad (3)$$

The densities of the three parts of Eq. (2) are $f_m \lambda_L$, $f_m(x_R - x_L)$, and $f_m \lambda_R$. Based on them, the rejection algorithm was constructed accordingly.^{1,3}

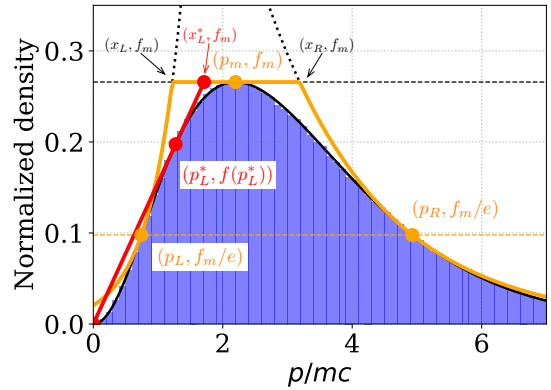


FIG. 1. The distribution function (black) of a Maxwell–Jüttner distribution with $t = 1$. The envelope function (orange) for the rejection method, the modified envelope (red), and Monte Carlo results (blue histogram) are presented.

Importantly, p_L and p_R are given as inputs. It was shown in Devroye¹ that the acceptance rate is highest when

$$f(p_L) = f(p_R) = \frac{f_m}{e} \quad (4)$$

Swisdak³ numerically obtained such solutions by using a root finder. This choice makes several terms simpler, as presented in Ref. 3.

^{a)}Electronic mail: seiji.zenitani@oeaw.ac.at

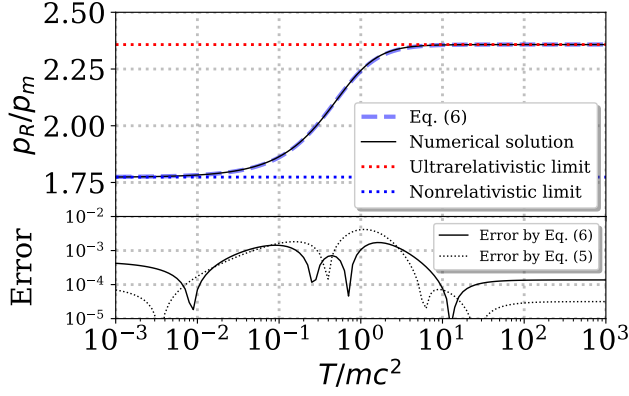


FIG. 2. Right e -folding position p_R , as a function of t . The bottom plot shows the relative errors of the two approximations on a log scale.

Next we present our modification. We propose the following approximations for the e -folding points,

$$p_L \approx \left(0.3017 + \frac{0.386}{4 + 3t + 4t^2} \right) p_m \quad (5)$$

$$p_R \approx \left(2.358 - \frac{1.168}{2 + 3t + 5t^2} \right) p_m \quad (6)$$

Below we explain how we derived them.

In the nonrelativistic limit of $t \rightarrow 0$, the distribution function and the mode are reduced to

$$f(p) = Ap^2 \exp\left(-\frac{1}{t} - \frac{p^2}{2t}\right), \quad p_m = \sqrt{2t} \quad (7)$$

By solving Eqs. (4) and (7), we find $p_L/p_m = \sqrt{-W_0(-e^{-2})} \approx 0.3977$ and $p_R/p_m = \sqrt{-W_{-1}(-e^{-2})} \approx 1.774$. Here, $W_0(x)$ and $W_{-1}(x)$ are the upper and lower branches of the Lambert W function. In the ultrarelativistic limit of $t \rightarrow \infty$, they are asymptotic to

$$f(p) = Ap^2 \exp\left(-\frac{p}{t}\right), \quad p_m = 2t \quad (8)$$

Equations (4) and (8) give $p_L/p_m = -W_0(-e^{-1.5}) \approx 0.3017$ and $p_R/p_m = -W_{-1}(-e^{-1.5}) \approx 2.358$.

We assume that p_X/p_m ($X = L, R$) is approximated by a rational function of t :

$$\frac{p_X}{p_m} = \frac{a + bt + ct^2}{1 + qt + rt^2} \quad (9)$$

where a, b, c, q , and r are positive parameters. Its derivative is

$$\left(\frac{p_X}{p_m}\right)' = \frac{b - qa + 2(c - ra)t + (cq - br)t^2}{(1 + qt + rt^2)^2} \quad (10)$$

We assume that p_X/p_m changes slowly. By setting $b = cq/r$, we eliminate the second order term in the numerator. Then p_X/p_m monotonically increases/decreases

TABLE I. A modified algorithm with a linear slope

```

require: t
f(x) ≡ p2 exp(-√(1 + p2/t))
pm2 ← 2t(t + √(1 + t2)), fm ← f(pm)
(pL*)2 ← ½(t2 + t√(4 + t2)), xL* ← fm/f(pL*)pL*
pR ← (2.358 - 1.168/(2 + 3t + 5t2))pm
λR ← -f(pR)/f'(pR), xR ← pR + λR log(f(pR)/fm)
S ← xR - ½xL* + λR
qL ← xL*/2S, qR ← λR/S, qC ← 1 - qL - qR
repeat
generate X1, X2 ~ U(0, 1)
if X1 < qL then // Left slope
p ← xL*√(X1/qL)
if pX2 ≤ f(p)xL*/fm break
else if X1 ≤ qL + qC then // Central box
p ← xL* + (xR - xL*)((X1 - qL)/qC)
if X2 ≤ f(p)/fm break
else // Right tail
U ← (X1 - qC - qL)/qR
p ← xR - λR log U
if UX2 ≤ f(p)/fm break
endif
end repeat
generate X3, X4 ~ U(0, 1)
px ← p(2X3 - 1)
py ← 2p√(X3(1 - X3)) cos(2πX4)
pz ← 2p√(X3(1 - X3)) sin(2πX4)

```

from a at $t = 0$ to c/r in the $t \rightarrow \infty$ limit,

$$\frac{p_X}{p_m} = \frac{c}{r} + \frac{a - (c/r)}{1 + qt + rt^2}. \quad (11)$$

The two limits a and c/r are set to the asymptotic values, discussed earlier. Once they are given, we search for q and r . We assume that q and r are fractions, to keep the final equations simple. Considering these issues, we obtain Eqs. (5) and (6) by trial and error.

The top portion of Fig. 2 compares Eq. (6) and the numerical solution of the right e -folding point p_R , as a function of t . The bottom portion shows the relative error between Eq. (6) and p_R , and also the relative error between Eq. (5) and p_L . Note that the numerical solutions are obtained by a root finder (the `scipy.optimize.fsolve` function in Python), whose tolerance is $\approx 1.5 \times 10^{-8}$. These plots show that Eqs. (6) and (5) are very good approximations. Meanwhile, since these approximations do not guarantee Eq. (4), the logarithmic terms in Eq. (3) should be retained, but Devroye¹'s original procedure works.

Next, we present our second modification. As shown by the red line in Fig. 1, we replace the left tail by a

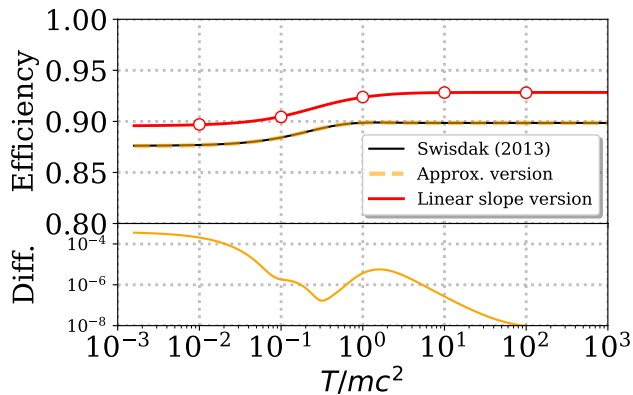


FIG. 3. Acceptance efficiencies of the original Swisdak method (black), the approximate version (orange), and the final version with the linear slope (Table I; red). The red circles indicate Monte Carlo results. The bottom panel shows the difference between the original method and the approximate method.

linear slope in the envelope function ,

$$F^*(p) = \begin{cases} f_m \left(\frac{p}{x_L^*} \right) & (p \leq x_L^*) \\ f_m & (x_L^* < p \leq x_R) \\ f(p_R) \exp \left(-\frac{p - p_R}{\lambda_R} \right) & (x_R < p) \end{cases} \quad (12)$$

The slope touches the distribution function at $(p_L^*)^2 = \frac{1}{2}(t^2 + t\sqrt{4+t^2})$, obtained from $\frac{\partial}{\partial p}(f(p)/p) = 0$. The slope meets the maximum line at $x_L^* = \{f_m/f(p_L^*)\}p_L^*$. Its relative position x_L^*/p_m monotonically changes from $(2/e)^{1/2} \approx 0.858$ ($t \rightarrow 0$) to $(2/e) \approx 0.738$ ($t \rightarrow \infty$). It is easy to generate a triangle-shaped distribution for the left part of Eq. (12), by using a random variate. The partial densities of Eq. (12) are $\frac{1}{2}f_m x_L^*$, $f_m(x_R - x_L^*)$, and $f_m \lambda_R$, and then the rejection scheme can be constructed, accordingly. A formal algorithm is presented in Table I. For completeness, a procedure to scatter p in three dimensions is added to the last part, so that the algorithm is self-contained. In practice, we can use Eq. (1) with $A = 1$, because the algorithm is independent of A .

We have generated a Maxwell–Jüttner distribution of 10^6 particles with $t = 1$, using the final algorithm with the linear slope. The results are shown by the blue histograms in Fig. 1, in agreement with the distribution (the black curve). This demonstrates that the proposed meth-

ods are ready to use in PIC and Monte Carlo simulations. The top portion of Fig. 3 compares theoretical acceptance rates of the original Swisdak method, the approximate version with Eqs. (5) and (6), and the linear-slope version in Table I. As already reported,³ the Swisdak method gives 88–90%. The approximate version gives very similar results, thanks to the good approximations of the e -folding points. This is evident in the (absolute) error in the bottom portion of Fig. 3. The acceptance rate of the linear-slope version is

$$\frac{1}{f_m(x_R - \frac{1}{2}x_L^* + \lambda_R)} = 90\text{--}93\%. \quad (13)$$

This prediction is confirmed by Monte Carlo tests with 10^6 particles, shown in open circles. The efficiency is improved by a few percent, because the linear slope bounds the distribution better. These three versions are as efficient as today’s leading methods.⁴ By comparing Fig. 3 with Fig. 9 in Ref. 4, the reader will see that they are very competitive in acceptance efficiency.

The proposed modifications are moderate, and would be rewarded by the numerical cost of the root finder and by the better acceptance efficiency.

ACKNOWLEDGEMENTS

The author acknowledges Marc Swisdak for discussion.

CONFLICT OF INTEREST

The author has no conflicts to disclose.

DATA AVAILABILITY

A Jupyter notebook is available at <https://doi.org/10.5281/zenodo.13274577>.

¹L. Devroye, *Non-Uniform Random Variate Generation*, Springer-Verlag (1986), Chap. 7, pp. 298–302, available at <http://luc.devroye.org/rnbookindex.html>.

²F. Jüttner, “Das Maxwellsche Gesetz der Geschwindigkeitsverteilung in der Relativtheorie,” *Ann. Phys.* **339**, 856 (1911).

³M. Swisdak, “The generation of random variates from a relativistic Maxwellian distribution,” *Phys. Plasmas* **20**, 062110 (2013).

⁴S. Zenitani, and S. Nakano, “Loading a relativistic Kappa distributions in particle simulations,” *Phys. Plasmas* **29**, 113904 (2022).